Bulletin of the Geological Society of Malaysia, Volume 68, December 2019, pp. 25 – 36
DOI : https://doi.org/10.7186/bgsm68201902

Paleoweathering, paleoenvironment and paleoclimate of the Nanka sandstone, Anambra basin, Nigeria

Henry Y. Madukwe

Department of Geology, Ekiti State University, Ado-Ekiti, Nigeria
E-mail address: henry.madukwe@eksu.edu.ng

Abstract: The paleoweathering, paleoclimate and paleoenvironment of the Nanka sandstone of the Anambra basin have been evaluated based on geochemical data. The Chemical Index of Alteration (CIA), Chemical Index of Weathering (CIW), Plagioclase Index of Alteration (PIA), Mineralogical Index of Alteration (MIA) and the A-CN-K ternary plot indicates intense weathering. Also, Rb/Sr, Al/K, Rb/K ratios are high while Sr/Ba is low indicating that the sediments were derived during intense chemical weathering of the source area. The Th/U-Th plot suggests that weathering conditions were not constant during sedimentation. The K_2O/Al_2O_3 ratio reveal that Nanka sandstone has minimal K-feldspar. There is negative correlation between CIA with K and Na+Ca; as weathering intensity increases, these elements are depleted, while there is a linear negative correlation between CIA and Al which implies high intensity of chemical weathering and subsequent formation of clay minerals. The paleoenviromental indices (U/Th, Ni/Co, Cu/Zn, (Cu+Mo)/Zn, V/Sc, V/Ni, V/Cr ratios, Mn*, Fe/Al, plot of Ni versus V, plot of V/Cr against Ni/Co, Mo concentrations and Ce/Ce*) and paleoclimate results suggest that the Nanka sandstone was deposited under oxic conditions with a humid climate on low relief in a non-marine deltaic environment and the paleosalinity based on low Sr/Ba ratio indicates low saline water during deposition in a continental environment.

Keywords: Nanka, paleoclimate, weathering, paleoenviroment, Index of Alteration

INTRODUCTION

The geochemistry of clastic sediments is the product of interacting factors including provenance, sorting, weathering and tectonism (Johnsson, 1993; McLennan *et al*., 1993). Major elements, trace elements and rare earth elements (REEs) and their elemental ratios are sensitive indicators of the source rocks, tectonic setting, paleoweathering conditions and paleoclimate of the clastic sedimentary rocks (Bakkiaraj *et al*., 2010). The Chemical Index of Alteration, the Plagioclase Index of Alteration, Chemical Index of Weathering and the Mineralogical Index of Alteration can be used to evaluate the source area weathering. The Anambra basin lies between latitudes 5.0°N and 8.0°N and longitudes 6.3°E and 8.0°E. The basin is roughly triangular in shape and covers an area of about 40,000 square kilometers with sediment thickness of 9 km and embodied by vast lithological heterogeneity in both horizontal and vertical extensions derived from a variety of paleo-environmental milieus (Akaegbobi, 2005). Anambra Basin in the south-eastern part of Nigeria (Figure 1) is one of the intracratonic basins in Nigeria whose origin is related to the separation of Africa from South America and the opening of South Atlantic Ocean (Ofoegbu, 1982). The theory of the evolution of the basin have been discussed by some authors (Obi,

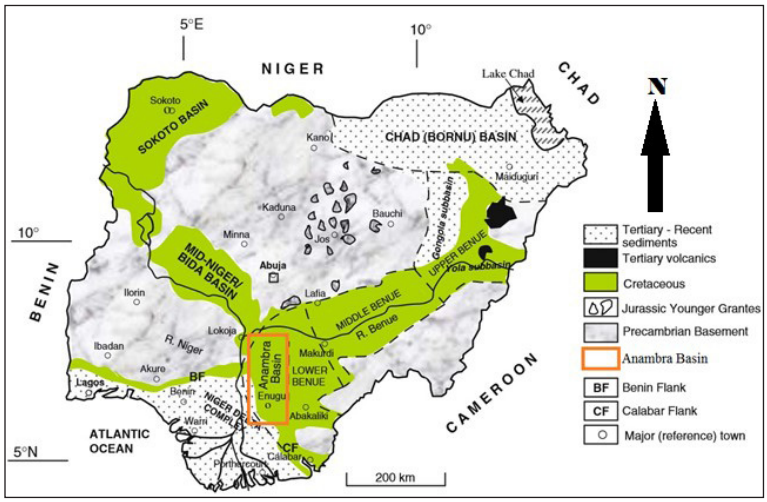

Figure 1: Schematic geological map of Nigeria showing the Basement Complex, Younger granites, and sedimentary basins (modified from Obaje, 2009)

2000). Subsequent evolution of the basin was influenced by some tectonic movements and the weight of accumulating sediments. Lithospheric thinning varying between 11.0 km and 27.0 km in a northeast southwesterly direction, while the thickness of the thermal lithosphere varies from 110 km to 128 km in a similar trend (Ekine & Onuoha, 2008). Sediment loading which contributed about 43% of the total subsidence was identified as the dominant factor for subsidence particularly in the southwestern and deeper parts of the basin, whereas thermal subsidence accounts for a greater part of the total subsidence in the north northeastern parts and about an average of 33% of the total subsidence (Ekine & Onuoha, 2008). The basin is situated west of the lower Benue Trough and often considered newest formation from the Benue Trough (Obaje, 2009). The Basin is bordered to the north by Bida Basin and Northern Nigeria Massif, to the East by Benue Trough, to the west by West African Massif and to the south by the Niger Delta Complex; it is bounded to the south by the Niger Delta Basin hinge line (Shirley & Gordian, 2013). According to Agagu & Adighije (1983) the Anambra basin has sediment thickness of about 12,000 m in its thickest part comprising mainly sandstones, shales, limestones and coal seams. Ola-Buraimo & Akaegbobi (2013b) invalidated earlier conception that Anambra Basin is exclusively of post-Santonian sediments. They showed that pre-Santonian sediments as old as Albian in age are present in the basin, which were dated based on palynology. The Asu-River Group is the oldest facies (in the basin) dated Albian to Lower Cenomanian. This is overlain by Eze-Aku Formation dated Upper Cenomanian to Turonian age; further overlain by the Awgu Formation dated as Coniacian (Ola-Buraimo, 2013a). Table 1 is an outline of the stratigraphy of the Anambra basin; Figure 2 shows the location map of the study area while Figure 3 is a generalised geology map of the basin. The stratigraphy of the Anambra basin has been examined by workers like Ola-Buraimo & Akaegbobi (2012); Ola-Buraimo (2013a, 2013b).

The Eocene stage was characterized by regressive phase that led to deposition of Ameki Group (Obi, 2000).

Table 1: Correlation chart for Early Cretaceous strata in southeastern Nigeria. (After Nwajide, 1990).

AGE	ABAKALIKI-ANAMBRA BASIN	AFIKPO BASIN
Oligocene	Ogwashi-Asaba Formation	Ogwashi-Asaba Formation
Eocene	Ameki/Nanka Formation/Nsugbe sandstone (Ameki sroup)	Ameki Formation
Paleocene	Imo Formation Nsukka Formation	Imo Formation Nsukka Formation
Maastrichtian	Ajalli Formation Mamu Formation	Ajalli Formation Mamu Formation
Campanian	Nkporo/Owelli Formation/Enugu shale	Nkporo shale/Afikpo sandstone
Santonian		
Coniacian	Agbani sandstone/ Awgu shale	Non-deposition/erosion
Turonian	Eze Aku Group	Eze Aku Group (include Amasiri sandstone)
Cenomanian-Albian	Asu River Group	Asu River Group
Aptian Barremian Hauterivian	Unnamed Group	
PRECAMBRIAN BASEMENT COMPLEX		

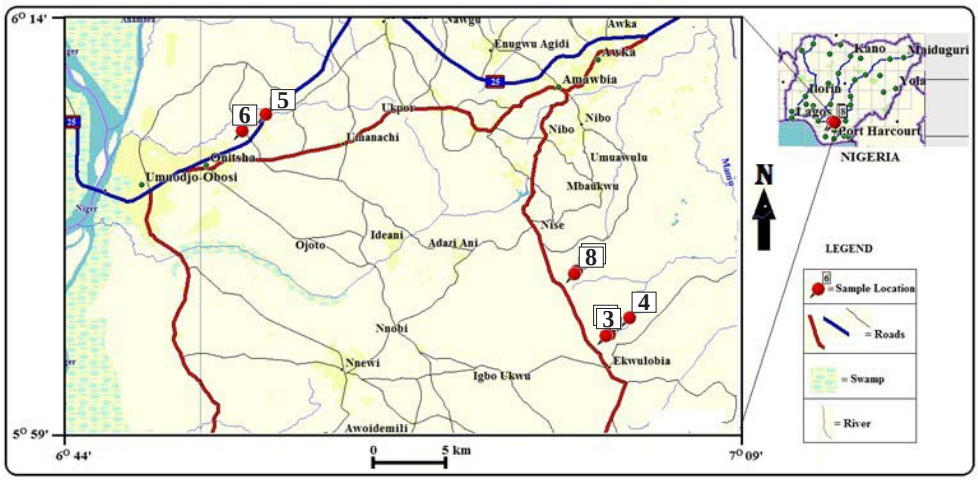

Figure 2: Location of the study and sampling areas.

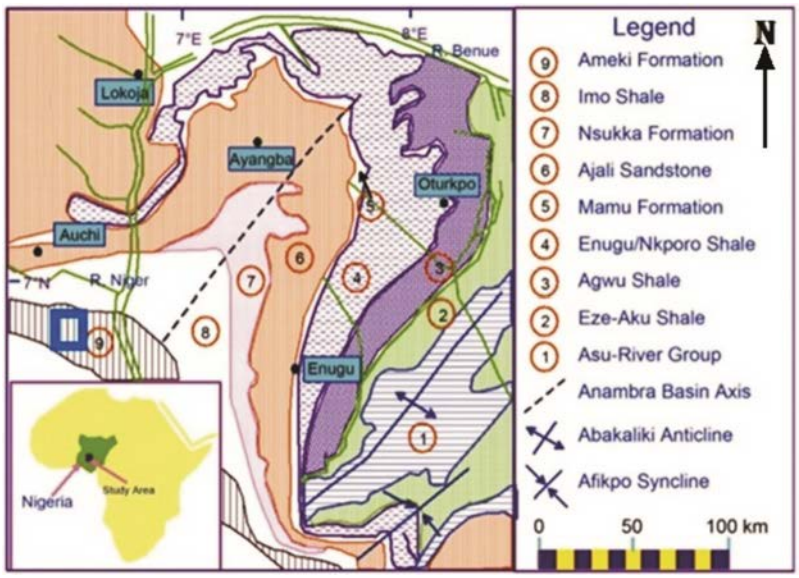

Figure 3: Geological map of the Anambra basin showing the various lithologies and study area (box) (modified from Nton & Bankole, 2013).

The Ameki Group comprises the Ameki Formation; Nanka Formation and the Nsugbe Formation. The Eocene to Recent sediments is mainly represented in the southern parts of the basin where thicker columns of the Paleocene Imo Shales are encountered (Ekine & Onuoha, 2008). Nwajide (1979, 1980) established the Nanka Formation as the loose sand facies of the Ameki Group, that is flaser-bedded, fine to medium grained with few mudrock breaks (Nwajide, 2013). The Nanka Sands have been described by Nwajide (1979). This research is aimed at using major, trace and rare earth elements geochemistry to explicate the source area weathering, paleoenvironment and paleoclimate of the Nanka sandstone in the Anambra basin.

METHODOLOGY

The study area lies within latitudes 6°02.568'N and 6°10.189'N and longitudes 7°51.116' E and 7°05.743' E. The area delineated for the present study stretches through Onitsha, Agulu, Oko, Nanka, Ekwulobia and Ogbunike all in Orumba Local Government Area, Anambra State. A thorough and careful traversing by foot was carried out and the location of different rock types outcropping in the areas studied noted. This was achieved with the aid of a Global Positioning System (G.P.S.). Also, useful information on locations of outcrops and easy accessibility to the locations was made possible by the villagers. However, the field operation involved visual observation of rocks at outcrops of interest and recorded in the field note book. Fresh samples were properly labeled to avoid mix-up before keeping them in the sample bags and taken for further study. Twenty (20) samples were collected altogether, but ten (10) of these were pre-analyzed, weighed, packaged and sent for geochemical analyses (major oxides, trace and rare earth elements) using X-ray Fluorescence (XRF) and LA-ICP-MS at Stellenbosch University, South Africa. Pulverised sandstone samples were analysed for major element using Axios instrument (PANalytical) with a 2.4 kWatt Rh X-ray Tube. The detailed procedures for sample preparation for the analytical technique are reported below.

Fusion bead method for Major element analysis:

- Weigh 1.0000 g ± 0.0009 g of milled sample
- Place in oven at 110 °C for 1 hour to determine H_2O
- Place in oven at 1000 ºC for 1 hour to determine LOI
- Add 10.0000 g ± 0.0009 g Claisse flux and fuse in M4 Claisse fluxer for 23 minutes
- 0.2 g of $NaCO_3$ was added to the mix and the sample+flux+$NaCO_3$ was pre-oxidized at 700 °C before fusion
- Flux type: Ultrapure Fused Anhydrous Li-Tetraborate-Li-Metaborate flux (66.67 % $Li_2B_4O_7$ + 32.83 % $LiBO_2$) and a releasing agent Li-Iodide (0.5 % LiI).

The result returned eleven major elements, reported as oxide percent by weight (SiO_2, TiO_2, Al_2O_3, Fe_2O_3, MgO, MnO, CaO, Na_2O, K_2O, SO_3 and P_2O_5). Loss on Ignition (LOI) is a test used in XRF major element analysis which consists of strongly heating a sample of the material at a specified temperature, allowing volatile substances to escape or oxygen is added, until its mass ceases to change. The LOI is made of contributions from the volatile compounds of H_2O, OH-, CO_2, F-, Cl-, S; in parts also K+ and Na+ (if heated for too long); or alternatively added compounds O_2 (oxidation, e.g. FeO to Fe_2O_3), later CO_2 (CaO to $CaCO_3$). In pyro-processing and the mineral industries such as lime, calcined bauxite, refractories or cement manufacturing industry, the loss on ignition of the raw material is roughly equivalent to the loss in mass that it will undergo in a kiln, furnace or smelter. The trace and rare elemental data for this work was acquired using Laser Ablation inductively coupled plasma spectrometry (LA-ICP-MS) analyses. The analytical procedures are as follows: the laser was used to vaporize the surface of the solid sample, while the vapour, and any particles, were then transported by the carrier gas

flow to the ICP-MS. The detailed procedures for sample preparation for both analytical techniques are reported below. Pressed pellet method for Trace element analysis:

- Weigh 8 g ± 0.05 g of milled powder
- Mix thoroughly with 3 drops of Mowiol wax binder
- Press pellet with pill press to 15-ton pressure
- Dry in oven at 100 ºC for half an hour before analysing.

The petrography of the sandstone samples was determined by point-counting each thin section.

PALEOWEATHERING

Table 2 is the result of the major oxides, trace and rare earth elements concentrations of the Nanka sandstone samples. The degree of source area weathering recorded in sediments can be determined by the Chemical Index of Alteration, CIA (Nesbit & Young, 1982). This index can be calculated by: CIA = $\{Al_2O_3/(Al_2O_3 + CaO^* + Na_2O + K_2O)\}$ x 100 (molar contents, CaO* represents the amount of CaO in silicate fraction of the sample). According to Nesbitt & Young (1982), high values of CIA implies the removal of labile elements like Ca, Na, K relative to the static residual constituent (Al^{+3}) during weathering, while low values suggest near absence of chemical weathering and therefore reflects cool or arid condition. CIA values for unaltered plagioclase and K-feldspar are ≈ 50 and values of 100 indicates complete conversion of feldspars to clay minerals like gibbsite and kaolinite (Fedo *et al*., 1995). The CIA value of PAAS is quantified to range from 70 to 75 which is believed to represent low to moderate degree of weathering. CIA values for the Nanka sandstone range between 82.67% and 98.54%, with an average value of 92.37%. The higher CIA values suggest intense weathering. However, it has been argued that CIA may not directly reflect the paleo-weathering conditions especially in sediments with variable provenances.

Improved assessment of weathering conditions in source area utilized by many scholars are indices like the Chemical Index of Weathering (CIW) and Plagioclase Index of Alteration (PIA) (Fedo *et al*., 1995). Compared to the major indices suggested to examine chemical weathering only the CIW circumvents the problems related to the remobilization of potassium during diagenesis or metamorphism and does not incorporate potassium because it may be leached or accumulate in the residue during weathering.

The Chemical Index of Weathering can be evaluated in terms of the molecular percentage of the oxide components, using the formulae: CIW = $\{Al_2O_3/(Al_2O_3 + CaO^* + Na_2O)\}$*100 based on Harnois (1988). CIW index increases with the degree of depletion of Na and Ca in the sediment relative to the Al. The CIA and CIW are interpreted in similar way with values of 50 for unweathered upper continental crust and roughly 100 for highly weathered materials, with complete removal of alkali and alkaline-earth elements (McLennan *et al*., 1983; McLennan, 1993; Mongelli *et al*., 1996). The Nanka sandstone CIW value ranges between 91.35 and 99.3% (average = 97%), indicating high degree of weathering of the source materials. The intensity of the chemical weathering can also be estimated using the Plagioclase Index of Alteration (Fedo *et al*., 1995); in molecular proportions: PIA = $[(Al_2O_3 - K_2O)/(Al_2O_3 + CaO^* + Na_2O - K_2O)] \times 100$ where CaO* is the CaO residing only in the silicate fraction. The maximum PIA value is 100 for completely altered material and un-weathered plagioclase has a PIA value of 50. The PIA values for the Nanka sandstones ranged from 90.3-99.3% (average = 96.2%), also indicating high degree of weathering. The Mineralogical Index of Alteration (MIA) proposed by Voicu *et al*. (1997) is another weathering parameter calculated as: MIA = 2*(CIA-50). MIA values between 0 and 20% are designated as incipient, i.e. just starting; 20-40% (weak); 40-60% (moderate) and 60-100% as intense to extreme degree of weathering. MIA value is between 65.3% and 97.1% (Average = 87.4%), which indicates intense weathering condition.

The A-CN-K diagram in Figure 4 shows no parallelism to A-CN-K lines, rather the plots shows two clusters of data-point: one at the "A" apex indicating substantial loss of Ca, Na and K, and abundance of kaolinite and/or chlorite and another close to the illite area and suggests that the effect of weathering had proceeded to the stage of removal of alkali and alkaline earth elements from the clay minerals. The position of the samples on the A-CN-K diagram, as well as the corresponding CIA, CIW, PIA and MIA values indicate that these sediments were generated from a source area strongly affected by chemical weathering which results in the depletion of selectively leached elements from the weathering profiles (Nesbitt *et al*., 1980; Wronkiewicz & Condie, 1987). In Figure 5, most of the samples plotted in the illite zone, this implies that the key K_2O and Al_2O_3 bearing minerals are illite and most likely the decomposition

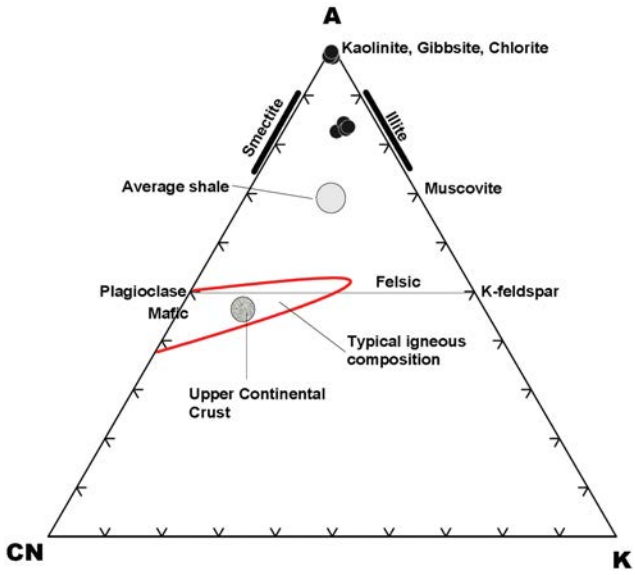

Figure 4: Ternary diagram showing the weathering trend of the studied samples (all in molar proportions); Al_2O_3–CaO +Na_2O–K_2O (A–CN–K). Fields from Gu *et al*. (2002).

Table 2: Major oxides (wt %) and trace elements (ppm) concentration of the Nanka sandstone.

Oxides	AG1	AG2	NA1	NA2	NA3	OG1	OG2	OK1	OK2	OK3	Average	UCC
SiO_2	92.42	93.82	94.35	94.68	95.33	97.18	94.66	96.58	97.78	93.95	95.08	65.89
Al_2O_3	3.91	3.55	3.19	2.94	2.32	0.38	2.68	1.30	0.50	2.63	2.34	15.17
Fe_2O_3	1.00	0.36	0.47	0.50	0.30	0.94	0.55	0.46	0.55	0.58	0.57	5
MnO	0.00	0.01	0.01	0.01	0.01	0.00	0.01	0.01	0.00	0.01	0.01	0.07
MgO	0.04	0.03	0.04	0.04	0.03	0.03	0.04	0.07	0.04	0.12	0.05	2.2
CaO	0.02	0.02	0.02	0.02	0.02	0.02	0.01	0.04	0.02	0.03	0.02	4.19
Na_2O	0.00	0.00	0.00	0.00	0.00	0.00	0.00	0.01	0.00	0.07	0.01	3.9
K_2O	0.02	0.04	0.02	0.01	0.01	0.04	0.01	0.14	0.06	0.32	0.07	3.39
TiO_2	0.23	0.19	0.14	0.20	0.11	0.07	0.19	0.17	0.03	0.15	0.15	0.5
P_2O_5	0.02	0.01	0.01	0.01	0.01	0.01	0.02	0.02	0.01	0.02	0.01	0.2
LOI	1.86	1.48	1.25	1.23	0.86	0.37	1.19	0.56	0.36	1.36	1.05	-
TRACE & RARE EARTH ELEMENTS												
V	20.75	11.31	8.20	13.90	7.51	9.57	13.05	11.90	6.54	13.10	11.58	107
Cr	26.10	14.55	18.40	59.50	17.90	15.15	22.05	13.35	7.20	25.25	21.95	85
Co	233.00	282.30	278.75	257.10	317.85	352.40	235.75	346.15	289.35	417.50	301.02	17
Ni	16.25	17.35	22.50	39.95	20.40	20.25	20.75	22.50	19.50	33.90	23.34	20
Cu	19.00	24.35	11.28	31.65	4.93	16.85	12.10	21.10	15.55	5.53	16.23	25
Zn	7.25	11.70	11.00	11.30	13.20	12.15	7.50	8.70	11.05	18.45	11.23	71
Zr	122.05	235.20	151.35	166.00	90.50	46.85	139.50	155.80	50.60	127.75	128.56	190
Nb	7.07	8.86	4.23	5.31	3.20	1.03	3.82	4.55	1.32	4.90	4.43	12.00
Mo	1.31	0.47	0.52	0.65	0.44	0.25	0.31	0.40	0.27	0.50	0.51	1.50
Hf	2.90	5.60	3.26	3.70	2.62	1.35	3.32	3.56	1.44	3.12	3.09	5.80
Ta	0.43	0.68	0.29	0.42	0.23	0.09	0.25	0.32	0.12	0.33	0.32	1.00
Rb	0.95	1.85	0.82	0.84	0.80	1.09	0.59	3.26	1.57	8.39	2.02	112.20
Sr	8.30	6.69	8.34	7.33	7.56	10.01	16.82	11.45	7.03	18.59	10.21	350
Cs	0.25	0.26	0.00	0.00	0.00	0.00	0.00	0.00	0.00	0.30	0.08	4.6
Ba	23.80	35.65	35.10	27.00	39.65	46.00	46.30	121.50	122.45	203.55	70.10	550
Pb	4.78	7.82	8.21	9.57	8.65	4.04	8.42	3.68	3.96	7.02	6.62	17
Th	2.87	3.40	1.82	2.88	1.14	0.89	2.40	1.86	1.05	1.72	2.00	10.7
U	0.84	0.93	0.59	0.70	0.47	0.28	0.49	0.40	0.31	0.54	0.56	2.8
Sc	10.42	9.23	8.40	8.61	8.14	7.02	8.49	9.26	8.46	8.57	8.66	13.60
Y	3.62	6.72	2.61	4.28	2.18	1.41	2.64	8.70	1.49	5.59	3.92	22
La	7.43	6.35	6.17	9.00	6.31	2.89	10.22	4.35	2.40	7.91	6.30	30
Ce	21.61	12.84	18.42	36.25	12.87	5.37	17.77	15.07	5.19	60.05	20.54	64
Pr	1.24	1.52	0.97	1.50	1.27	0.55	1.77	1.00	0.50	1.63	1.20	7.10
Nd	3.51	5.31	3.29	5.65	4.68	2.08	6.72	4.46	1.89	6.24	4.38	26
Sm	0.67	1.09	0.46	1.04	0.79	0.35	0.94	0.83	0.43	1.37	0.80	4.5
Eu	0.11	0.21	0.06	0.19	0.22	0.06	0.18	0.20	0.08	0.30	0.16	0.88
Gd	0.38	1.10	0.59	1.02	0.52	0.22	0.68	0.98	0.31	1.47	0.73	3.8
Tb	0.11	0.19	0.10	0.17	0.09	0.05	0.12	0.20	0.05	0.21	0.13	0.64
Dy	0.59	1.11	0.50	0.74	0.53	0.25	0.56	1.39	0.39	1.11	0.72	3.5
Ho	0.11	0.26	0.11	0.18	0.11	0.05	0.12	0.33	0.09	0.21	0.16	0.8
Er	0.43	0.79	0.30	0.44	0.27	0.13	0.37	0.75	0.18	0.57	0.42	2.3
Tm	0.06	0.11	0.05	0.08	0.08	0.05	0.06	0.10	0.07	0.12	0.08	0.33
Yb	0.69	0.84	0.42	0.48	0.35	0.12	0.39	0.73	0.19	0.63	0.48	2.2
Lu	0.08	0.15	0.12	0.09	0.06	0.00	0.06	0.10	0.07	0.12	0.09	0.32

UCC: Upper Continental Crust (Taylor & McLennan, 1985; 1995)

of K-feldspars and muscovite during weathering and K remained fixed in clay. Some ratios such as Sr/Ba, Al/K, Ti/Na, Rb/K, Rb/Sr and K/Na have also been utilized to investigate the degree of weathering based on the premise that these elements usually display remarkable different mobility and are fractionated to diverse degrees during weathering (Sawyer, 1986; Ding *et al.*, 2001; Yang *et al.*, 2004; Roy *et al.*, 2008). High K/Na, Rb/Sr, Al/K, Rb/K, Ti/Na ratios and low Sr/Ba ratio indicate strong chemical weathering (Yang *et al.*, 2004). Na and Sr are more mobile than K, Al, Rb and Ba and consequently easily removed from parent rock during weathering. Both K and Rb are integrated into clay minerals by adsorption and cation exchange during initial weathering of fresh rocks. But with increasing weathering intensity, K is preferentially leashed compared to Rb (Wronkiewicz & Condie, 1989). In the present study, Rb/Sr, Al/K, Rb/K ratios are high while Sr/Ba is low indicating strong chemical weathering. Rb/K, Ak/K and Sr/Ba shows positive correlation with CIA values whereas Rb/Sr shows negative correlation with CIA. These suggest that ratios of Rb/K, Rb/Sr and Sr/Ba are controlled by the degree of weathering.

The K_2O/Al_2O_3 ratio reveal how much of alkali feldspar as against plagioclase and clay minerals present in the original rock. K_2O/Al_2O_3 ratios of the alkali feldspar ranges from 0.4 – 1; illite approximately 0.3 and other clay minerals nearly zero (Cox *et al*., 1995). K_2O/Al_2O_3 ratio greater than 0.5, suggests dominance of alkali feldspar as compared to other minerals in the original rock. In contrast those having K_2O/Al_2O_3 ratios of less than 0.4 suggest minimal alkali feldspar in the original rock (Cox *et al*., 1995). The K_2O/Al_2O_3 ratio of the Nanka sandstone ranges from 0.003 to 0.12 (average = 0.049), indicating that Nanka sandstone has minimal K-feldspar. Figure 6a and 6b shows a negative correlation between CIA with K and Na+Ca. As weathering intensity increases, these elements are depleted, while Figure 7 shows a strong correlation between CIA and Al which implies high intensity of chemical weathering and subsequent formation of clay minerals.

Some authors (Taylor & McLennan, 1985; McLennan *et al*., 1990, 1995; Gu *et al*., 2002) have used the Th/U ratio to interpret the weathering history due to the oxidation and loss of uranium during the weathering process. Some of the Nanka samples plotted above the upper crust limit while some plotted slightly below the upper crust mean value (Figure 8). The scenario suggests that weathering conditions were not constant during sedimentation. McLennan *et al*. (1995) suggested that a ratio near 3.8 indicates a relatively un-weathered source, but according to Pe-Piper *et al*. (2008), the precise value will vary according to local hinterland geology.

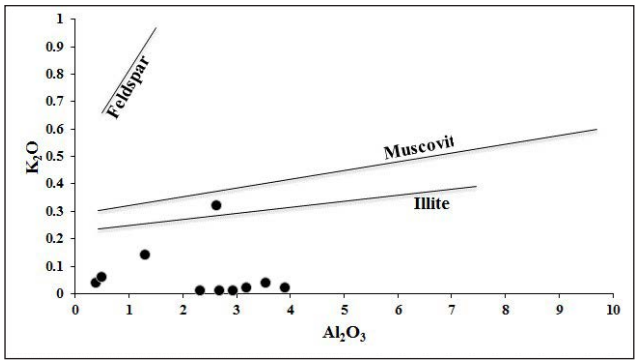

Figure 5: Al_2O_3 versus K_2O diagram showing the distribution of Nanka sandstones plotting in the illite zone (Cox *et al.,* 1995).

PALEOENVIROMENT AND PALEOCLIMATE

Oxidation and reduction states are significant for identifying sediment deposition in marine or non-marine environment. The accretion of some trace metals in sediments is directly or indirectly constrained by redox conditions via either a change in redox state and/or speciation (McKay *et al*., 2007). U/Th, Ni/Co, Cu/Zn, (Cu+Mo)/Zn, V/Sc and V/Cr ratios have been utilized to assess paleo-redox conditions (Bjorlykke, 1974; Hallberg, 1976; Dypvik, 1984; Dill, 1986; Shaw *et al*., 1990; Brumsack, 2006; Nagarajan *et al*., 2007; Hetzel *et al*., 2009). According to Jones & Manning (1994), U/Th ratio is higher in organic rich mudstones compared to sandstones; U/Th ratios below 1.25 suggest oxic conditions of deposition, while values above 1.25 indicate suboxic and anoxic conditions (Hallberg, 1976; Jones & Manning, 1994). The U/Th values for the Nanka sandstone is between 0.20 and 0.41 (average = 0.29), which indicates an oxic environment.

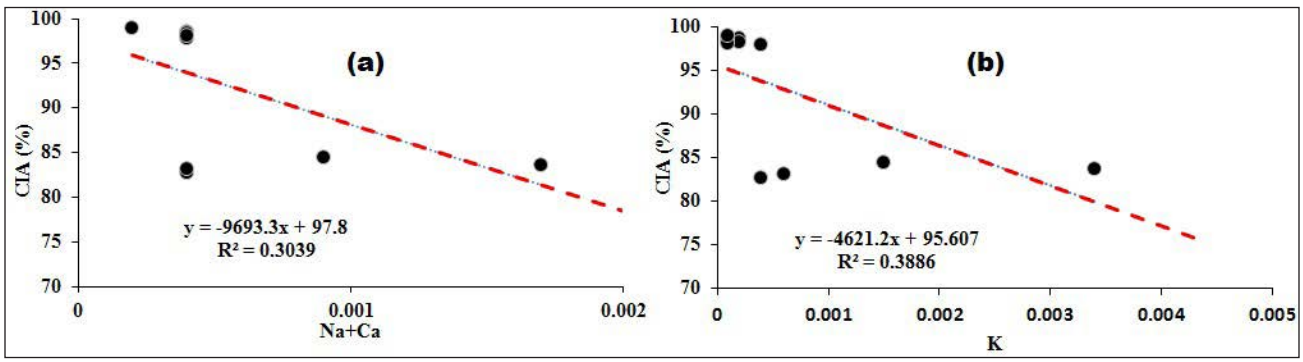

Figure 6: (a) Correlation between CIA and Na+Ca, (b) between CIA and K.

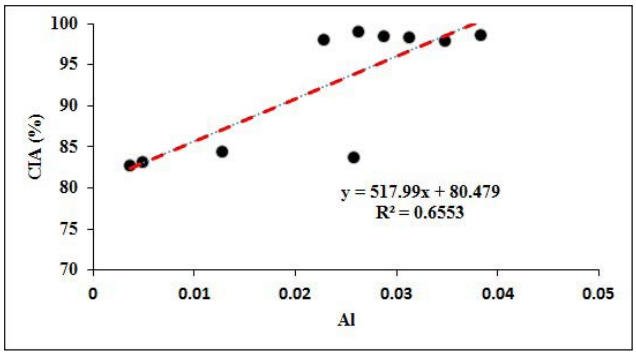

Figure 7: Positive correlation between CIA and Al.

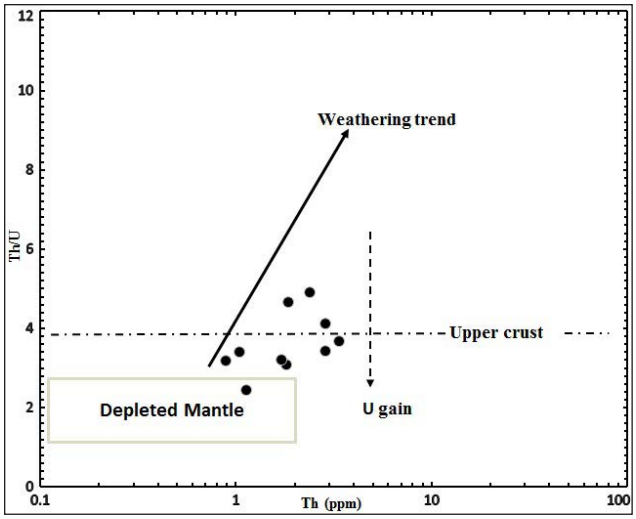

Figure 8: Th/U vs. Th plot for the Nanka sandstone. Fields and trends from Gu *et al.* (2002).

V accumulates relative to Ni in reducing environments, where sulphate reduction is more efficient. Ni is mainly enriched in organic-rich sediments where these metals are trapped with organic matter (Leventhal & Hosterman, 1982; Gilkson *et al*., 1985). The proportionality of these two elements V/(V+Ni) is significant to outline evidence on Eh, pH and sulphide activity in the depositional environment (Madhavaraju & Lee, 2009). V/(Ni+V) ratios below 0.46 indicate oxic environments, but ratios between 0.54 and 0.82 suggest suboxic and anoxic environments (Hatch & Leventhal, 1992). The Nanka sandstone V/(Ni + V) values range from 0.25 to 0.56 (Avg. = 0.33), which indicates oxic condition of deposition.

According to Jones & Manning (1994), the Ni/Co ratios below 5 indicate oxic environments, while ratios above 5 indicate suboxic and anoxic environments. The Ni/Co ratios for the Nanka sandstone range from 0.06 to 0.16 (average = 0.08), signifying an oxic environment. Molybdenum (Mo) has been used as a proxy for deciphering depositional conditions. Concentrations of Mo increases with increasing anoxic conditions (Alberdi-Genolet & Tocco, 1999; Piper, 1994; Crusius *et al*., 1996). Mo concentrations between 5 to 40 ppm can be used as an indicator of anoxic conditions and that less than 5 ppm indicating oxic conditions (Piper, 1994; Crusius *et al*., 1996). The concentration of Mo in the Nanka sandstone is between 0.25 and 1.31 ppm and this suggests an oxic conditions during deposition.

The ratio (Cu+Mo)/Zn is shown to be a relevant paleoredox indicator for bottom water and sediment surface. The (Cu+Mo)/Zn values for the Nanka sandstone range from 0.60 to 6.06 (average = 3.62), which suggests oxic to suboxic environment of deposition. High Cu/Zn ratios indicate reducing depositional conditions, while low Cu/Zn ratios suggests oxidising conditions (Hallberg, 1976); the Cu/Zn ratios for the studied samples is between 0.30-2.80 (average = 1.60), indicating oxic to suboxic; but more oxidising conditions. According to Lewan (1984), the relative proportions of V and Ni are controlled by the depositional environment. V/Ni ratio less than 1.9 indicate deposition under oxic conditions; ratios ranging between 1.9 and 3 indicate suboxic conditions and greater than 3 indicates deposition in a reducing environment; (Galarraga *et al*., 2008). The V/Ni ratios for the samples range from 0.34-1.28 (average = 0.54) indicating deposition under oxic condition.

According to Hetzel *et al*. (2009), the V/Sc ratios below 9.1 imply oxic depositional environment. V/Sc values for the Nanka sandstone range from 0.77 and 1.99 (average = 1.32) suggesting oxic depositional environment. V/Cr ratio has been utilized as an index of paleooxygenation due to the incorporation of Cr in the detrital fraction of sediments and its possible substitution for Al in the clay structure (Kimura & Watanabe, 2001). Vanadium solubility in natural waters, its extraction from seawater and absorption onto sediments are predominantly affected by redox conditions (Bellanca *et al*., 1996). Vanadium may be bound to organic matter by the addition of V^{4+} into porphyrins, and is generally found in sediments deposited in reducing environments (Kimura & Watanabe, 2001). V/Cr ratios above 2 indicate anoxic conditions, while values below 2 suggest more oxidizing conditions (Jones & Manning, 1994). The V/Cr values for sandstone under investigation range between 0.23 and 0.91 (average = 0.62), which points to deposition in an oxic environment.

The Mn* value is a significant paleochemical indicator of the redox conditions of the depositional environment (Bellanca *et al*., 1996; Cullers, 2002; Machhour *et al*., 1994). The expression for calculating Mn* value is $Mn^* = \log[(Mn_{sample}/Mn_{shales})/(Fe_{sample}/Fe_{shales})]$, where the values used for the Mn_{shales} and Fe_{shales} are 600×10^{-6} and 46150×10^{-6}, respectively (Wedepohl, 1978). The reduced iron and manganese form different solubilities of compounds across a redox boundary, while manganese tends to accumulate in more oxygenated conditions above the redox boundary (Bellanca *et al*., 1996). The Nanka sandstone has Mn* values ranging from -0.05 to 0.24 (average = 0.06), this suggests oxic depositional environment.

Rare earth elements like Cerium (Ce) have been used as redox proxies. Ce has two oxidation states: Ce^{3+} and Ce^{4+}, and both depend on the prevalent redox condition; fractionation

of Ce relative to its proximate elements is a direct response to the variability in oxidation state (De Baar *et al*., 1988). In oxic marine environments, Ce^{4+} preponderates and is utilised by strongly reactive Fe-Mn-oxyhydroxides, leading to depletion of Ce in oxic seawater. Cerium anomaly (Ce/Ce*) may be utilised to determine the paleoenvironmental of deposition. Values >1 suggests an oxidizing environment (Piper, 1974; Milodowski & Zalasiewicz, 1991; McDaniel *et al*., 1994). The Nanka sandstone has Ce/Ce* values ranging between 1.01 and 4.10 with an average of 1.72 indicating an oxic environment of deposition.

Sr and Ba are regarded as indicators of paleosalinity (Liu *et al*., 1984; Deng & Qian, 1993; Wang, 1996). A high Sr/Ba ratio reflects high salinity, and a low Sr/Ba ratio indicates low salinity (Deng & Qian 1993). The Nanka sandstone has Sr/Ba values between 0.09 and 0.36 (average = 0.21), indicating low saline water during deposition and a strong continental rather than marine influence under oxic conditions. Figure 9 is a plot of Fe/Al ratios against the sample points, which shows almost all the samples plotting in the oxic zone, also Figures 10 and 11 show the samples plotting in the oxic zones.

The degree of chemical weathering is a function of climate and rates of tectonic uplift (Wronkiewicz & Condie, 1987). According to Jacobson *et al*. (2003), the increasing chemical weathering intensity implies decrease in tectonic activity and/or the change of climate towards warm and humid conditions which are more auspicious for chemical weathering in the source region. The applicability of the ratios of $SiO_2/(Al_2O_3+K_2O+Na_2O)$ for paleoclimatic condition (Suttner & Dutta, 1986) during deposition of sediments in the basin is well acknowledged by several workers. Figure 12 shows all the samples plotting in humid to semi-humid climatic conditions, which reflects paleoclimatic condition during the deposition of Nanka sandstone. Figure 13 is another paleoclimatic bivariate log plot by Suttner & Dutta (1986) showing the samples plotting in the humid and semi-humid zone, this paleoclimatic condition will influence increase mineral instability.

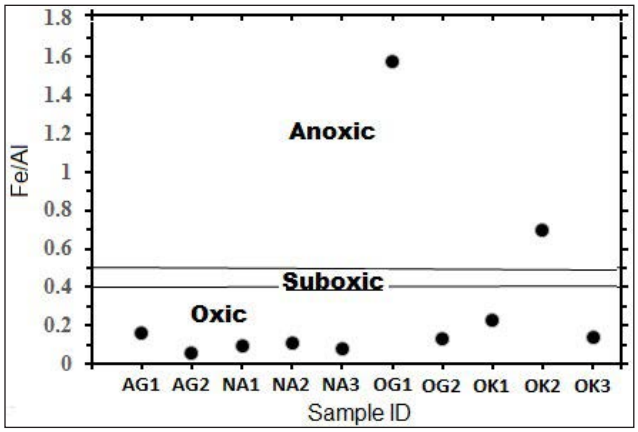

Figure 9: Fe/Al (molar) in the Nanka sandstone (adapted from Lyons & Severmann, 2006; Algeo & Maynard, 2008).

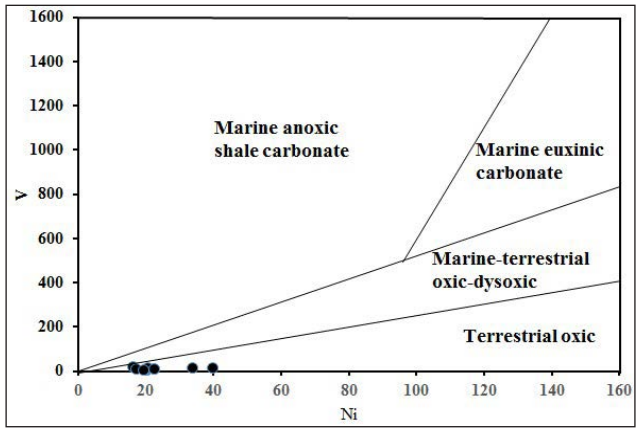

Figure 11: Cross-plot of vanadium versus nickel of the Nanka sandstone samples showing that the sandstone had mainly terrigenous source input and were deposited under oxic conditions (modified after Galarraga *et al*., 2008).

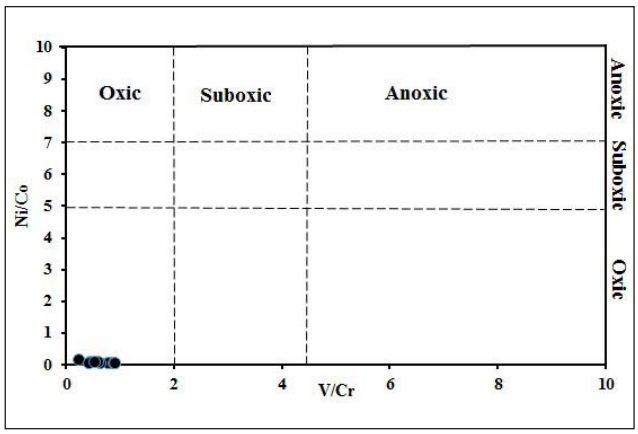

Figure 10: Cross-plot of Ni/Co versus V/Cr of the analysed samples showing that the sandstone was deposited under oxic conditions (after Jones & Manning, 1994).

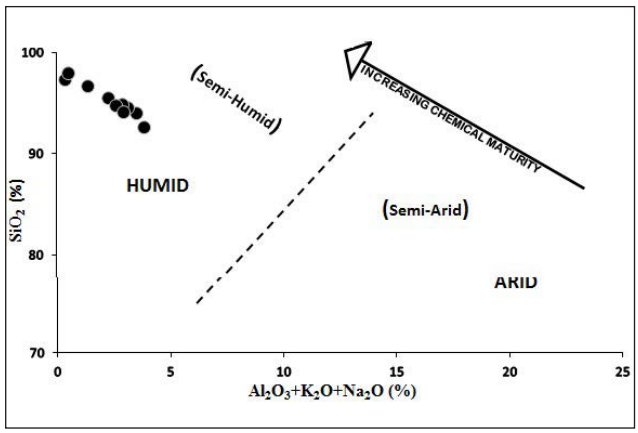

Figure 12: Bivariate plot of SiO_2 vs. $(Al_2O_3 + K_2O + Na_2O)$ to discriminate paleoclimatic condition during the deposition of the Eocene sediments (after Suttner & Dutta, 1986).

Figure 14 shows the Nanka sandstone as originating from a metamorphic source rock under humid climate conditions. This particular diagram can discriminate only sources of metamorphic and plutonic rocks (humid or arid conditions) and does not discriminate between different tectonic settings. Figure 15 is based on Weltje *et al*. (1998); the Nanka sandstone plotted in zone 4, indicating deposition on low plains with a tropical humid condition. From Figure 16, the Nanka sandstone is identified as non-marine and deltaic sandstones. The aforementioned paleoenviromental and paleoclimatic results suggest that the Nanka sandstone was deposited in oxic non-marine conditions. The depositional environment of the Nanka sandstone can also be categorised based on the ternary diagram of Englund & Jorgensen (1973). This involves chemical classification on the basis of (Al_2O_3) - $(K_2O + Na_2O + CaO)$ - $(Fe_2O_3 + MgO)$ contents (AKF). Figure 17 shows the samples plotting in the continental zone indicating a non-marine deltaic setting.

CONCLUSIONS

All the paleo-weathering indices of the Nanka sandstone indicate that the sediments were derived during intense chemical weathering of the source area. The sandstone has minimal K-feldspar, and weathering conditions were

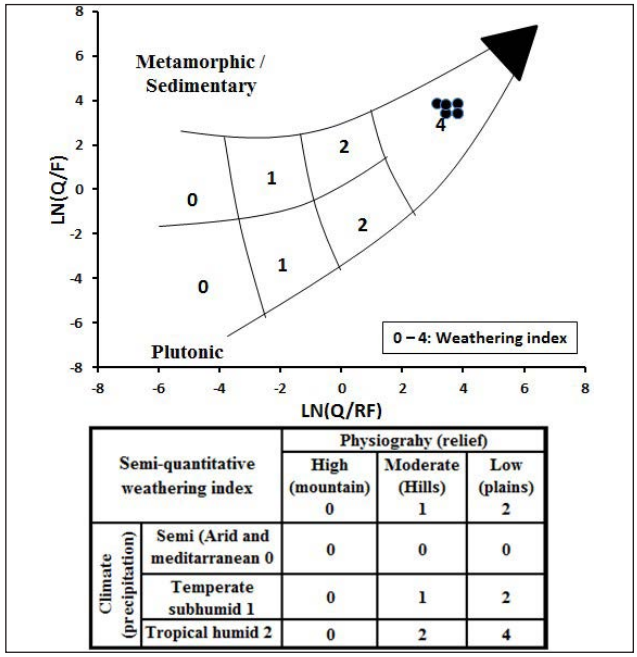

Semi-quantitative weathering index		Physiography (relief) High (mountain) 0	Moderate (Hills) 1	Low (plains) 2
Climate (precipitation)	Semi (Arid and meditarranean 0	0	0	0
	Temperate subhumid 1	0	1	2
	Tropical humid 2	0	2	4

Figure 15: Log-ratio plot after Weltje *et al*. (1998). Q: quartz, F: feldspar, RF: rock fragments. Fields 1-4 refer to the semi-quantitative weathering indices defined on the basis of relief and climate as indicated in the table.

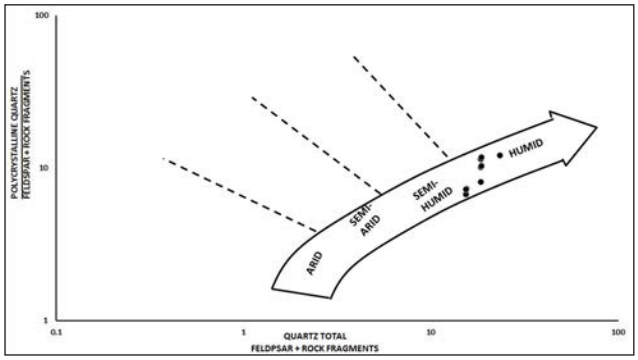

Figure 13: Bivariate log/log plot of the ratio of polycrystalline to feldspar plus rock fragments against the ratio of total quartz to feldspar plus rock fragments (after Suttner & Dutta, 1986).

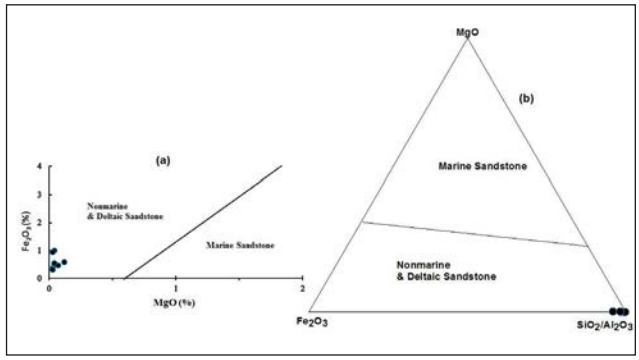

Figure 16: Binary (a) and ternary (b) diagrams showing characterization and differentiation of marine from non-marine sandstones. The Nanka sandstones plotted in the non-marine and deltaic field (after Ratcliffe *et al*., 2007).

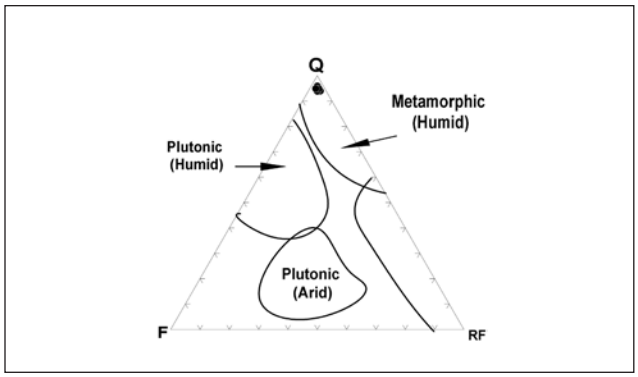

Figure 14: Q-F-R plot of the Nanka sandstone indicating paleoclimate of the source (after Suttner *et al*., 1981).

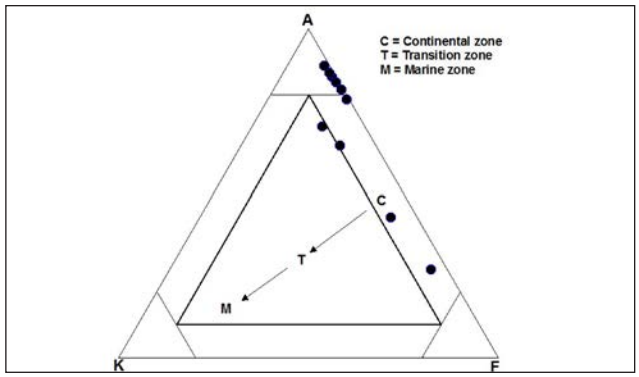

Figure 17: (Al_2O_3) - (K_2O+Na_2O+CaO) - (Fe_2O_3+MgO) A-K-F Ternary diagram for the Nanka sandstone (modified from Englung & Jorgensen, 1973).

not constant during sedimentation. The paleoenviromental parameters points to deposition under oxic conditions with low salinity in non-marine deltaic environment. The paleoclimate analyses indicate that the Nanka sandstone was deposited on low relief with tropical humid climate that increases mineral instability.

ACKNOWLEDGEMENTS

The author acknowledges the assistance of the final year students (2016/2017 session) who participated in the fieldwork and also Dr A.B. Eluwole for preparation of the location map.

This research did not receive any specific grant from funding agencies in the public, commercial, or not-for-profit sectors.

REFERENCES

Agagu, O. K. & Adighije, C. I., 1983. Tectonic and sedimentation framework of the lower Benue Trough, Southern Nigeria. Journal of African Earth Science, 1, 267-274.

Akaegbobi, M.I., 2005. Sequence Stratigraphy of Anambra Basin: Journal of African Earth Sciences, 42, 394-406.

Alberdi-Genolet, M. & Tocco, R., 1999. Trace metals and organic geochemistry of the Machiques Member (Aptiana-Albian) and La Luna Formation (Cenomanian-Campanian), Venezuela. Chemical Geology, 160, 19-38.

Algeo, T.J. & Maynard, J.B., 2008. Trace-metal covariation as a guide to water-mass conditions in ancient anoxic marine environments. Geosphere, 4(5), 872-887.

Bakkiaraj, D., Nagendra, R., Nagarajan, R., & Armstrong-Altrin, J. S., 2010. Geochemistry of sandstones from the Upper Cretaceous Sillakkudi Formation, Cauvery Basin, Southern India: Implication for provenance. Journal of the Geological Society of India, 76, 453-467.

Bellanca, A., Claps, M., Erba, E., Masetti, D., Neri, R., Premolisilva, I., & Venezia, F., 1996. Orbitally induced limestone/marlstone rhythms in the Albian-Cenomanian Cismon section (Venetian region, northern Italy): Sedimentology, calcareous and siliceous plankton distribution, elemental and isotope geochemistry". Paleogeography, Paleoclimatology and Paleoecology, 126, 227-260.

Bjorlykke, K., 1974. Geochemical and mineralogical influence of Ordovician island arcs on epicontinental clastic sedimentation: a study of Lower Palaeozoic sedimentation in the Oslo region, Norway. Sedimentology, 21(2), 251-272.

Brumsack, H. J., 2006. The trace metal content of recent organic carbon-rich sediments: implications for Cretaceous black shale formation. Palaeogeography, Palaeoceanography, Palaeoecology, 232 (2-4), 344-361.

Cox, R., Lowe, D.R. & Cullers, R.L., 1995. The influence of sediment recycling and basement composition on evolution of mudrock chemistry in the southwestern United States. Geochimica et Cosmochimica Acta, 59, 2919-2940.

Crusius, J., Calvert, S., Pedersen, T. & Sage, D., 1996. Rhenium and molybdenum enrichments in sediments as indicators of oxic, suboxic and sulfidic conditions of deposition. Earth and Planetary Science Letters, 145, 65-78.

Cullers, R.L., 2002. Implications of elemental concentrations for provenanace, redox conditions, and metamorphic studies of shales and limestones near Pueblo, Co, USA. Chemical Geology, 191, 305-327.

De Baar, H.J.W., German, C.R., Elderfield, H., & van Gaans, P., 1988. Rare-earth element distributions in anoxic waters of the Cariaco Trench. Geochimica et Cosmochimica Acta, 52(5), 1203-1219.

Deng, H.W. & Qian, K., 1993. Analysis on sedimentary geochemistry and environment. Science Technology Press, Gansu, 15-85 (in Chinese).

Dill, H., 1986. Metallogenesis of early Paleozoic graptolite shales from the Graefenthal Horst (northern Bavaria-Federal Republic of Germany. Economic Geology, 81, 889-903.

Ding, Z.L., Sun, J.M., Yang, S.L. & Liu, T.S., 2001. Geochemistry of Pliocene red clay formation in the Chinese Loess Plateau and implications for its origin, source provenance and palaeoclimatic change. Geochimica et Cosmochimica Acta, 65, 905-913.

Dypvik, H., 1984. Geochemical compositions and depositional conditions of Upper Jurassic and Lower Cretaceous Yorkshire clays. England. Geological Magazine, 121(5), 489-504.

Ekine, A.S. & Onuoha, K.M., 2008. Burial history analysis and subsidence in the Anambra Basin, Nigeria. Nigerian Journal of Physics, 20 (1), 145-154.

Englund, J.O., & Jorgensen, P., 1973. A chemical classification system for argillaceous sediments and factors affecting their composition. Geol. Stockholm Forh., 95, 87-97.

Fedo. C.M, Nesbitt, H.W. & Young, G.M., 1995. Unraveling the effects of potassium metasomatism in sedimentary rocks and paleosols, with implications for paleoweathering conditions and provenance. Geology, 23, 921-924.

Galarraga, F., Reategui, K., Martïnez, A., Martínez, M. M., Llamas, J. & Márquez, G., 2008. V/Ni ratio as a parameter in palaeoenvironmental characterisation of nonmature medium-crude oils from several Latin American basins. Journal of Petroleum Science and Engineering, 61, 9-14.

Gilkson, M., Chappell, B.W., Freeman, R.S. & Webber, E., 1985. Trace elements in oil shales, their source and organic association with particular reference to Australian deposits. Chemical Geology, 53, 155-174.

Gu, X.X., Liu, J.M., Zheng, M.H., Tang, J.X., & Qt, L., 2002. Provenance and Tectonic setting of the Proterozoic turbidites in Hunan, South China: Geochemical Evidence. Journal of Sedimentary Research, 72, 393-407.

Hallberg, R.O., 1976. A Geochemical Method for Investigation of Paleoredox Conditions in Sediments. Ambio Special Report, 4, 139-147.

Harnois, L., 1988. The CIW index: A new chemical index of weathering. Sedimentary Geology, 55, 319-322.

Hatch, J. R. & Leventhal, J. S., 1992. Relationship between inferred redox potential of the depositional environment and geochemistry of the Upper Pennsylvanian (Missourian) Stark Shale Member of the Dennis Limestone, Wabaunsee County, Kansas, U.S.A. Chemical Geology, 99, 65-82.

Hetzel, A., Böttcher, M. E., Wortmann, U. G. & Brumsack, H., 2009. Paleo-redox conditions during OAE 2 reflected in Demerara Rise sediment geochemistry (ODP Leg 207). Palaeogeography, Palaeoclimatology, Palaeoecology, 273, 302-328.

Jacobson, A.D., Blum, J.D., Chamberlian, C.P., Craw, D. & Koons, P.O., 2003. Climate and tectonic controls on chemical weathering in the New Zealand Southern Alps. Geochimica et Cosmochimica Acta, 37, 29-46.

Johnsson, M.J., 1993. The system controlling the composition of clastic sediments. Geological Society of America (Special

Paper), 284, 1-19.

Jones, B. & Manning, D. A. C., 1994. Comparison of geological indices used for the interpretation of palaeoredox conditions in ancient mudstones. Chemical Geology, 111, 111-129.

Kimura, H. & Watanabe, Y., 2001. Oceanic anoxia at the Precambrian-Cambrian boundary. Geology, 21, 995-998.

Leventhal, J.S. & Hosterman, J.W., 1982. Chemical and mineralogical analysis of Devonian black-shale samples from Martin County, Kentucky; Carroll and Washington counties, Ohio; Wise County, Virginia; and Overton County, Tennessee, U.S.A. Chemical Geology, 37, 239-264.

Lewan, M.D., 1984. Factors controlling the proportionality of vanadium to nickel in crude oils. Geochimica et Cosmochimica Acta, 48, 2231-2238.

Liu, Y.J., Cao, L.M., Li, Z.L., Wang, H.N., Chu, T.Q. & Zhang, J.R., 1984. Elements of geochemistry. Science Press, Beijing, 283-372 (in Chinese).

Lyons, T.W. & Severmann, S., 2006. A critical look at iron paleoredox proxies: New insights from modern euxinic marine basins. Geochimica et Cosmochimica Acta, 70(23), 5698-5722.

Machhour, L., Philip, J. & Oudin, J.L., 1994. Formation of laminate deposits in anaerobic-dysaerobic marine environments. Marine Geology, 117, 287-302.

Madhavaraju, J. & Lee, Y.I., 2009. Geochemistry of the Dalmiapuram Formation of the Uttatur Group (Early Cretaceous), Cauvery Basin,southeastern India: Implications on provenance and paleo-redox conditions. Revista Mexicana de Ciencias Geológicas, 26, 380-394.

McDaniel, D.K., Hemming, S. R., Mclennan, S.M. & Hanson, G.N., 1994. Resetting of neodymium isotopes and redistribution of REE'S during sedimentary processes: The early Proterozoic Chelmsford formation, Sudbury Basin, Ontario, Canada. Geochimaet Cosmochimica Acta, 58, 931-941.

McKay, J.L., Pedersen, T.F. & Mucci, A., 2007. Sedimentary redox conditions in continental margin sediments (N.E. Pacific)—Influence on the accumulation of redox-sensitive trace metals. Chemical Geology, 238, 180-196.

McLennan, S.M., 1993. Weathering and global denudation. Journal of Geology, 101, 295-303.

McLennan, S.M., Taylor, S.R. & Eriksson, K.A., 1983. Geochemistry of Archean shales from the Pilbara Supergroup, Western Australia. Geochim. Cosmochim. Acta, 47, 1211-1222.

McLennan, S.M., Taylor, S.R., McCulloch, M.T. & Maynard, J.B., 1990. Geochemical and Nd-Sr isotopic composition of deep-sea turbidites: crustal evolution and plate tectonic associations. Geochemica et Cosmochimica Acta, 54, 2015-2050.

McLennan, S.M., Hemming, S., McDaniel, D.K. & Hanson, G.N., 1993. Geochemical approaches to sedimentation, provenance, and tectonics. In: Johnson, M.J. and Basu, A. (Eds.), Processes Controlling the Composition of Clastic Sediments. Geological Society of America Special Paper, 284, 21-40.

McLennan, S.M., Hemming, S.R., Taylor, S.R. & Eriksson, K.A., 1995. Early Proterozoic crustal evolution: Geochemical and Nd-Pb isotopic evidence from metasedimentary rocks, southwestern North America. Geochimica et Cosmochimica Acta, 59, 1159-1177.

Milodowski, A.E. & Zalasiewkz, J.A., 1991. Redistribution of rare earth elements during diagenesis of eurbidice /hemipelagic mudrock sequences llandovery age from central Wales. In: A.C. Mortan, S.P. Todd and P.D.W. Houghton (Eds.), Geological Society London Special Publications, 57, 101-124.

Mongelli, G., Cullers, R.L. & Muelheisen, S., 1996. Geochemistry of Late Cretaceous-Oligocenic shales from the Varicolori Formation, southern Apennines, Italy: implications for mineralogical, grain-size control and provenance. Eur. J. Mineral., 8, 733-754.

Nagarajan, R., Madhavaraju, J., Nagendral, R., Armstrong-Altrin, J.S. & Moutte, J.S.J., 2007. Geochemistry of Neoproterozoic shales of the Rabanpalli Formation, Bhima Basin, Northern Karnataka, southern India: implications for provenance and paleoredox conditions. Revista Mexicana de Ciencias Geológicas, 24(2) 150-160.

Nesbitt, H.W. & Young, G.M., 1982. Early Proterozoic climates and plate motions inferred from major element chemistry of lutites. Nature, 299, 715-717.

Nesbitt, H.W., Markovics, G. & Price, R.C., 1980. Chemical processes affecting alkalines and alkaline earths during continental weathering. Geochim. Cosmochim. Acta, 44, 1659-1666.

Nton, M.E. & Bankole, S.A., 2013. Sedimentological characteristics, provenance and hydrocarbon potential of post Santonian sediments in Anambra Basin, southeastern Nigeria. RMZ-Materials and Geoenvironment Journal, 60(1), 47-66.

Nwajide, C.S., 1979. A lithostratigraphic analysis of the Nanka sand, Southeastern Nigeria. Nigerian Journal of Mining and Geology, 16, 103-109.

Nwajide, C.S., 1980. Eocene tidal sedimentation in the Anambra Basin, Southern Nigeria. Sedimentary Geology, 25, 189-207.

Nwajide, C. S., 1990. Cretaceous sedimentation and palaeogeography of the Central Benue Trough. In: Ofoegbu, C.O. (Ed.), The Benue Trough, Structure and Evolution. Friedr. Vieweg and Sohn, Braunchweig/Wiesbaden, 19-38.

Nwajide, C.S. & Reijers, T.J.A., 1996. Sequences architecture in outcrops, examples from the Anambra Basin, Nigeria. Nigerian Association of Petroleum Explorationists Bulletin, 11(1), 23-32.

Nwajide, C.S. & Reijers, T.J.A., 1997. Sequence architecture of the Campanian Nkporo and Eocene Nanka Formations of the Anambra Basin, Nigeria. Nigerian Association of Petroleum Explorationists Bulletin, 12(1), 75-87.

Nwajide, S.C., 2013. Geology of Nigeria's Sedimentary Basins. CSS Bookshops, Lagos. 565 p.

Obaje, N. G., 2009. Geology and Mineral Resources of Nigeria (Lecture Notes in Earth Sciences 120). Springer-Verlag, Berlin Heidelberg. 221 p.

Obi, G.C., 2000. Depositional Model for the Campanian Maastrichtian Anambra Basin, Southern Nigeria [Ph.D. Thesis]. University of Nigeria, Nsukka, Nigeria. 299 p.

Ofoegbu, C., 1982. Evolution of Anambra Basin. Nigerian Journal of Mining and Geology, 5(6), 45-60.

Ola-Buraimo, A.O., 2013a. Palynological stratigraphy of the Upper Cenomanian-Turonian Eze-Aku Formation in Anambra Basin, southeastern Nigeria. Journal of Biological and Chemical Research, 30(1), 54-67.

Ola-Buraimo, A.O., 2013b. Biostratigraphy and paleoenvironment of the Coniacian Awgu Formation in Nzam-1 well, Anambra Basin, southeastern Nigeria. International Journal of Scientific and Technology Research, 2(3), 112-122.

Ola-Buraimo, A.O. & Akaegbobi, I.M., 2012. Neogene dinofagellate cyst assemblages of the late Miocne-Pliocene Ogwashi-Asaba sediment in Umuna-1 well, Anambra Basin, southeastern Nigeria. Journal of Petroleum and Gas Exploration Research, 2(6), 115-124.

Ola-Buraimo, A.O. & Akaegbobi, I.M., 2013a. Palynological and paleoenvironmental investigation of the Campanian-lowermost

Maastrichtian Asata/Nporo shale in the Anambra Basin, southeastern Nigeria. British Journal of Applied Sciences and Technology, 3(4), 898-915.

Ola-Buraimo, A.O. & Akaegbobi, I.M., 2013b. Palynological evidence of the oldest (Albian) sediment in Anambra Basin, southeastern Nigeria. Journal of Biological and Chemical Research, 30(2), 387-408.

Pe-Piper, G., Triantafyllidis, S. & Piper, D.J.W., 2008. Geochemical identification of clastic sediment provenance from known sources of similar geology: The Cretaceous Scotian Basin, Canada. Journal of Sedimentary Research, 78, 595-607.

Piper, D.Z., 1974. Rare earth elements in the sedimentary cycle: A summary. Chemical Geology, 14, 285-304.

Piper, D.Z., 1994. Seawater as the source of minor elements in black shales, phosphorites and other sedimentary rocks. Chemical Geology, 114, 95-114.

Ratcliffe, K.T., Morton, A.C., Ritcey, D.H. & Evenchick, C.A., 2007. Whole-rock geochemistry and heavy mineral analysis as petroleum exploration tools in the Bowser and Sustut basins, British Columbia, Canada. Bulletin of Canadian Petroleum Geology, 55(4), 320-336.

Roy, P.D., Caballeroa, M., Lozanoc, R. & Sykatz-Klossd, W., 2008. Geochemistry of Late Quaternary sediments from Tecocomulco Lake, central Mexico: Implication to chemical weathering and provenance. Chemie der Erde, 68, 383-393.

Sawyer, E.M., 1986. The influence of source rock type, chemical weathering and sorting on the geochemistry of clastic sediments from Quetico metasedimentary belt, Superior Province, Canada. Chemical Geology, 55, 77-95.

Shaw, T. J., Geiskes, J. M. & Jahnke, R. A., 1990. Early diagénesis in differing depositional environments: the response of transition metals in pore water. Geochimica et Cosmochimica Acta, 54(5), 1233-1246.

Shirley, O. O. & Gordian, C. O., 2013. Sedimentology and sequence stratigraphy of the Nkporo Group (Campanian–Maastrichtian), Anambra Basin, Nigeria. Department of Geology, Anambra State University, Uli, Nigeria.

Suttner, L.J. & Dutta, P.K., 1986. Alluvial sandstone composition and paleoclimate 1. Framework mineralogy. Journal of Sedimentary Petrology, 56, 326-345.

Suttner, L.J., Basu, A. & Mack, G.H., 1981. Climate and the origin of quartz arenites. Journal of Sedimentary Petrology, 51, 235-246.

Taylor, S.R. & McLennan, S.M., 1985. The Continental Crust: Its Composition and Evolution. Blackwell, Oxford. 312 p.

Taylor, S. R. & McLennan, S. M., 1995. The geochemical evolution of the continental crust. Rev. Geophys., 33, 241-265.

Voicu, G., Bardoux, M., Harnois, L. & Grepeau, R., 1997. Lithological and geochemical environment of igneous and sedimentary rocks at Omai gold mine, Guyana, South America. Exploration and Mining Geology, 6, 153-170.

Wang, A.H.. 1996. Discriminant effect of sedimentary environment by the Sr/Ba ratio of different existing forms. Acta Sedimentol. Sin., 14, 168-173.

Wedepohl, K.H., 1978. Manganese: Abundance in Common Sediments and Sedimentary Rocks, Handbook of Geochemistry. Springer, Berlin, 1-17.

Weltje, G.J., Meijer, X.D. & De Boer, P.L., 1998. Stratigraphic inversion of siliciclastic basin fills: a note on the distinction between supply signals resulting from tectonic and climatic forcing. Basin Research, 10, 129-153.

Wronkiewicz, D.J. & Condie, K.C., 1987. Geochemistry of Archean shales from the Witwatersrand Supergroup, South Africa: source-area weathering and provenance. Geochimica et Cosmochimica Acta, 51, 2401-2416.

Wronkiewicz, D.J. & Condie, K.C., 1989. Geochemistry and provenance of sediments from the Pongola Supergroup, South Africa: evidence for a 3.0-Ga-old continental craton. Geochimica et Cosmochimica Acta, 53, 1537-1549.

Yang, S.Y., Li, C.X., Yang, D.Y. & Li, X.S., 2004. Chemical weathering of the loess deposits in the lower Changiang Valley, China, and palaeoclimatic implications. Quaternary International, 117, 27-34.

Manuscript received 17 January 2019
Revised manuscript received 3 May 2019
Manuscript accepted 5 May 2019